# Ammonia IRMS-TPD Study on the Distribution of Acid Sites in Mordenite

**Miki Niwa,*,† Katsuki Suzuki,† Naonobu Katada,†,‡ Tomonori Kanougi,§ and Takashi Atoguchi§**

*Department of Materials Science, Faculty of Engineering, Tottori University 4-101, Koyama-minami, Tottori, 680-8552 Japan, PRESTO, Japan Science and Technology Agency, Kawaguchi 332-0012 Japan, and Polymer Laboratory, UBE Industries, Ltd., 8-1, Goi-minamikaigan, Ichihara, Chiba 290-0045 Japan*

*Received: March 14, 2005; In Final Form: June 10, 2005*

Using an IRMS-TPD (temperature programmed desorption) of ammonia, we studied the nature, strength, crystallographic location, and distribution of acid sites of mordenite. In this method, infrared spectroscopy (IR) and mass spectroscopy (MS) work together to follow the thermal behavior of adsorbed and desorbed ammonia, respectively; therefore, adsorbed species were identified, and their thermal behavior was directly connected with the desorption of ammonia during an elevation of temperature. IR-measured TPD of the $NH_4^+$ cation was similar to MS-measured TPD, thus showing the nature of Brønsted acidity. From the behavior of OH bands, it was found that the Brønsted acid sites consisted of two kinds of OH bands at high and low wavenumbers, ascribable to OH bands situated on 12- and 8-member rings (MR) of mordenite structure, respectively. The amount and strength of these Brønsted hydroxyls were measured quantitatively based on a theoretical equation using a curve fitting method. Up to ca. 30% of the exchange degree, $NH_4^+$ was exchanged with $Na^+$ on the 12-MR to arrive at saturation; therefore, in this region, the Brønsted acid site was situated on the large pore of 12-MR. The $NH_4^+$ cation was then exchanged with $Na^+$ on 8-MR, and finally exceeded the amount on 12-MR. In the 99% $NH_4$-mordenite, Brønsted acid sites were located predominantly on the 8-MR more than on the 12-MR. Irrespective of the $NH_4^+$ exchange degree, the strengths $\Delta H$ of Brønsted OH were 145 and 153 kJ $mol^{-1}$ on the 12- and 8-MR, respectively; that is, the strength of Brønsted acid site on the 8-MR was larger than that on the 12-MR. A density functional theory (DFT) calculation supported the difference in the strengths of the acid sites. Catalytic cracking activity of the Brønsted acid sites on the 8-MR declined rapidly, while that on the 12-MR was remarkably kept. The difference in strength and/or steric capacity may cause such a difference in the life of a catalyst.

## Introduction

Brønsted acidity in the framework of zeolites is a matter of importance for fundamental and industrial investigations. It is known that the acid site ($H^+$) of a zeolite is generated by the isomorphous substitution of $Si^{4+}$ in the silicate framework by $Al^{3+}$. Many techniques, for example, ammonia TPD (temperature-programmed desorption) using MS (mass spectroscopy),[1,2] confirmed that the number of acid sites was principally equal to that of aluminum atoms inside the zeolite framework. Quantitative agreement between the numbers of acid sites and the framework aluminum was, in the early stage of this investigation, limited to siliceous zeolites with less than 1.5 mol/kg of acid site; however, after a precise study using $NH_4$-type zeolites, it was extended to Y-type zeolites with a high concentration of acid sites.[3] $NH_4$-type zeolites retain the structure, and after removing ammonia, an in situ prepared H-type zeolite shows the number of acid sites equal to the aluminum cation in the framework, as long as it is kept unexposed to the outside humidity.[4]

Also, the strength of acid sites of zeolites is important to interpret their catalytic property. It has been clarified that the average strength of a zeolite is dependent on its crystal structure. It is possible to study the zeolite acidity from the quantum chemical calculation.[5−7] With the help of these advanced techniques, global understanding on solid acidity is now in progress. For a complete understanding of zeolite acidity, the acid strength of each crystallographically specific site should be determined experimentally.

It has been known previously that mordenite has a very strong acid site. Its ammonia adsorption heat, ca. 150 kJ $mol^{-1}$, measured by ammonia TPD is greater than that of any other studied zeolites.[1,2] Mordenite looks like a zeolite that has acid sites with relatively homogeneous strength; however, the distribution of the acidity has been investigated. There are four kinds of T sites, named $T_1-T_4$, as shown in Figure 1; four oxygen atoms bond with the Al in each T site and hydroxyls direct toward 8- or 12-member rings. As mentioned below, however, OH positioned in the small side pockets of four and five-member rings is unknown. Totally, 10 kinds of oxygen exist in the framework of mordenite and therefore 10 kinds of Brønsted acid sites are structurally possible. The location of Al in the mordenite was studied by Alberti,[8,9] and the distribution of Brønsted acid sites has been studied by IR (infrared) spectroscopy using $NH_3$,[10] pyridine,[11] $N_2$,[12] and CO [13] as probes, individually or comprehensively.[14]

In this paper, we study the acidic property of mordenite using IRMS-TPD of ammonia, a new technique for characterization in which IR and MS work together and the site and strength of

* Corresponding author. E-mail: mikiniwa@chem.tottori-u.ac.jp. Tel and fax: +81-857-31-5256.
† Tottori University.
‡ Japan Science and Technology Agency.
§ UBE Industries, Ltd..

10.1021/jp051304g CCC: $30.25 
Published on Web 09/20/2005

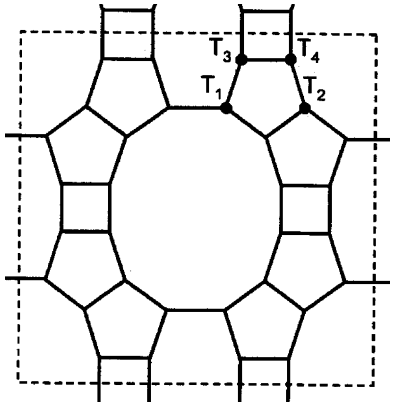


**Figure 1.** Structure of mordenite.

Brønsted OH bands are clearly revealed.[15] From the comparison of MS-TPD with IR-TPD, the thermal behavior of ammonia adsorbed on each OH group can be observed. Thus, with this method, we can get an insight into the nature of Brønsted acid sites in detail.

## Experimental Method

**IRMS-TPD.** IR (Perkin-Elmer Spectrum-One) and MS (Pfeiffer QME200) were connected with a vacuum line to which helium was allowed to flow as a carrier. The experimental apparatus is described elsewhere in detail.[15] To avoid a delay in the desorbed ammonia arriving at the MS, we selected a rapid flow rate (vide infra); at the selected standard conditions, helium was allowed to flow into the line kept at 25 Torr (1 Torr = 0.133 kPa) with 125 mL $min^{-1}$. An IR beam was transmitted to the self-compressed disk (about 8 mg and 10 mm in diameter). After evacuation of the sample at 813 K, IR spectra were recorded before and after ammonia adsorption, shown as N($T$) and A($T$) ($T$, temperature in K), respectively, during the elevation of temperature from 373 to 873 K in a ramp rate of 10 K $min^{-1}$. The difference spectra, A($T$) − N($T$), were calculated to identify the adsorbed species and the OH band interacted with the species. A differential change in the absorption intensity with respect to the measured temperature, $-d\{A(T) - N(T)\}/dT$, was calculated at the selected wavenumber (hereafter, called IR-TPD) to compare with TPD measured by MS operating at $m/e$, 16.

**Zeolite Sample.** Na-form mordenite with $Si/Al_2 = 15$ (Reference Catalyst, Catalyst Society of Japan, JRC-Z-M15) was ion-exchanged with $NH_4NO_3$ and evacuated in the IR cell at 813 K as above. Five species of mordenite with various exchange degrees of $NH_4^+$ were prepared, and the composition was measured by ICP (inductively coupled plasma) spectroscopy after digestion in HF. Because the ammonium-type zeolite retains the finest conditions of solid acid sites, it was evacuated in the IR cell and the in situ prepared HNaM-15 was used for the IRMS-TPD measurement throughout the present study.

**Catalytic Reaction.** The cracking of octane was measured by a continuous flow method. Octane vapor mixed with nitrogen carrier gas (partial pressure of octane, 14 Torr) was allowed to flow into a Pyrex glass reactor heated at 673 K. A zeolite sample (0.03 g) was activated at 813 K in a dried $N_2$ flow for 1 h before the reaction. The products and reactant were fed into a gas chromatograph directly through a six-way valve and analyzed using a silicone capillary column and flame ionization detector.

**DFT Calculation.** DFT calculations were carried out, for all periodic models before and after $NH_3$ adsorption, by solving Kohn Sham equation self-consistently[16] as implemented in DMol$^3$ software.[17] The one-electron Schrödinger equations were solved only at the $k = 0$ wave-vector point of the Brillouin zone. Basis sets were represented by the numerical type atomic orbitals, and in this study double numerical with polarization (DNP) basis sets were employed. The Vosko−Wilk−Nusair (VWN) local correlation functional[18] was used in order to optimize geometries. The SCF (self-consistent field) convergence criterion was set to $10^{-5}$ Ha, and the gradient convergence criterion was set to $10^{-3}$ Ha/Bohr.

## Results

**Experimental Conditions for IRMS-TPD of Ammonia.** We have measured ammonia TPD for the characterization of acid sites under the following standard conditions[2]; 0.1 g of the sample, 60 mL $min^{-1}$ of the carrier gas flow rate and 100 Torr of the pressure inside the cell. However, the conditions were not appropriate for the present experiment of IRMS-TPD, because, due to the large volume and complex shape of in-situ IR cell, desorbed ammonia was delayed in arriving at the mass spectrometer; thus, an accurate comparison between TPD spectra measured by IR and MS was difficult. Therefore, a rapid flow rate of helium carrier gas was required to measure the profiles of ammonia adsorbed and desorbed correctly. However, too fast a flow rate (too large mass amount per time) of the carrier gas made the concentration of desorbed ammonia low, resulting in the difficulty in detecting ammonia by MS. After the TPD profiles were examined under various conditions, finally, the most suitable conditions were chosen (120 mL $min^{-1}$ of the carrier gas, 25 Torr of inside pressure, and ca. 0.008 g of the sample). In other words, TPD in the present study was measured with a contact time of 1/100 of that in our previous measurements.

When ammonia TPD is measured under conventional experimental conditions, it is controlled under the equilibrium between ammonia molecules in the gas phase and adsorbed on the sample.[1,2] Because the contact time of carrier gas was much shorter than that in previous experiments, the conditions must be examined to know whether ammonia molecules are in equilibrium. To do so, we examined a dependence of the temperature of desorbed peak (Tm) on the contact time of the carrier gas. Ammonia TPD was measured on the in situ prepared HM-15 by varying not only the flow rate of helium carrier gas but also the pressure inside the IR cell with the weight of the sample being kept 0.008 g. The peak temperature of ammonia desorption, measured by MS, shifted higher when increasing the contact time W/F, as shown in Figure 2. Figure 3 shows the relationship between the parameters derived from the theoretical equation;[19] the theory for TPD experiments controlled by the equilibrium between gaseous and adsorbed ammonia molecules predicts a linear relation between these parameters. A linear correlation was observed at the smaller values of 1/Tm, that is, at larger contact times, but it did not extend to the conditions (120 mL $min^{-1}$ of the flow rate and 25 Torr of the pressure inside the cell) that were chosen in the present study. This means that the TPD experiment in the present study was incompletely controlled by the equilibrium.

$\Delta H$ (enthalpy change by ammonia desorption, namely the heat of ammonia adsorption) on the in situ prepared HM-15 was determined using a linear portion of the plot in Figure 3 on the basis of a theoretical equation,[19] and it was determined as 153 kJ $mol^{-1}$, which was in agreement with the value reported previously.[1,2] $\Delta S$ (entropy change by ammonia desorption) could be calculated from the determined $\Delta H$ based on the theoretical equation. $\Delta S$ consists of $\Delta S$ upon phase transformation (i.e.,

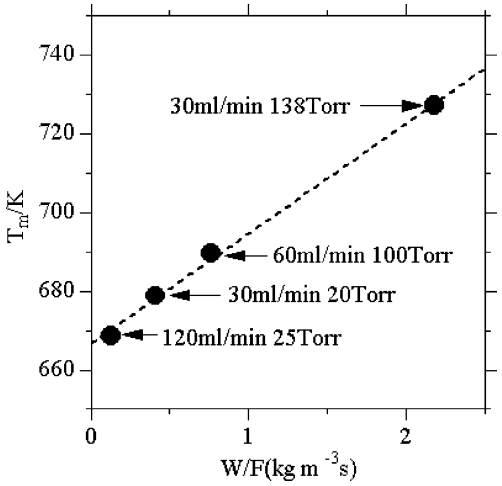


**Figure 2.** Dependence of peak maximum temperature on the experimental conditions (W/F).

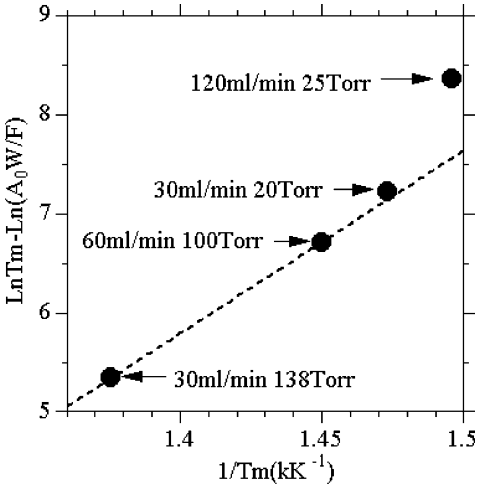


**Figure 3.** Plots for confirmation of TPD experiments controlled by the equilibrium between ammonia molecules in the gas phase and adsorbed on the solid.

desorption) and $\Delta S$ upon physical mixing with carrier gas helium. $\Delta S$ upon desorption was regarded as being almost the same as $\Delta S$ upon the vaporization of liquid ammonia, that is, 95 J K$^{-1}$ mol$^{-1}$ [1]. Therefore, $\Delta S$ upon physical mixing was determined to be 47 J K$^{-1}$ mol$^{-1}$. Thus, the determined value of $\Delta S$ is used in the present study (vide infra) to calculate the $\Delta H$ by the simulation of IR-TPD spectrum.

**Temperature Effect for OH Absorption Band.** To analyze the change in position, shape and intensity of the OH band by heating, before the adsorption of ammonia, we measured the IR spectra of in situ prepared HM-15 in a helium flow with increasing and decreasing the temperature. It was confirmed that the position, shape, and intensity of IR absorption of the OH band changed reversibly with the temperature. By raising the temperature, the peak shifted to the low wavenumber, and the absorbance decreased; and these changes occurred reversibly, as shown in Figure 4. Therefore, these changes should be corrected to analyze the difference spectra quantitatively. As shown in Figure 4, a linear relationship between the band position and measurement temperature was observed. From the slope of linear relationship, the change of band position with respect to difference in temperature was described as

$$\frac{\Delta\nu}{\Delta T} = -0.056 \text{ cm}^{-1} \text{ K}^{-1} \quad (1)$$

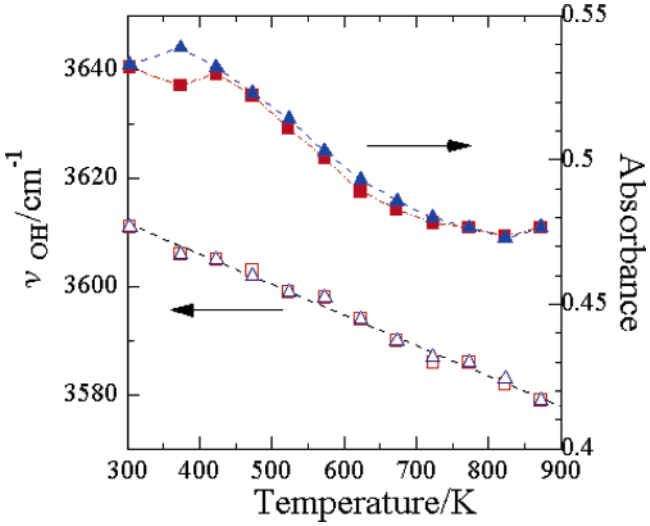


**Figure 4.** Change of OH band position and absorbance with the temperature on in situ prepared HM-15 in which the temperature was increased (square) or decreased (triangle).

where $\Delta\nu$ and $\Delta T$ are differences in wavenumber and temperature, respectively. The wavenumbers of difference spectra are therefore corrected into the values which should be observed at 373 K using eq 1. After the correction, the change in shape of the OH band with the measurement temperature became small enough to neglect (vide infra).

However, the change of absorbance in Figure 4 from 500 to 700 K could be described by a following equation, when $\Delta A$ denoted the difference in absorbances

$$\frac{\Delta A}{\Delta T} = -2 \times 10^{-4} \text{ K}^{-1} \quad (2)$$

However, the rate of recovery of OH band intensity by increasing the temperature, $(-\text{d}\{\text{A}(T) - \text{N}(T)\}/\text{d}T$, i.e., IR-TPD) was ca. $4 \times 10^{-3}$ K$^{-1}$ at the peak maximum and therefore considerably higher than the temperature dependence in eq 2 (vide infra). In the IRMS-TPD, furthermore, not an absolute value of absorbance but the difference in absorbances before and after ammonia adsorption is utilized for the analysis. Therefore, the temperature effect on the absorbance is, more or less, canceled. The absorbance is therby used without correction.

**IRMS-TPD on the In Situ HM-15 ($NH_4^+$, 99% Exchange Level).** Figure 5 shows the difference spectra of ammonia on the in situ prepared HM-15. After the adsorption of ammonia, at 373 K, a strong absorption ascribable to the bending vibration of the $NH_4^+$ cation was observed at 1430 cm$^{-1}$. NH stretching vibration was characteristically observed in the broad range of 3400−2500 cm$^{-1}$.[20] However, a negative change of the peak intensity was observed in the OH region; obviously, this is because the $NH_4^+$ cation was formed on the Brønsted OH. Elevating the temperature reduced the intensities of positive bands of the adsorbed species and recovered the OH bands.

We calculated IR-TPD from changes in the intensities of these bands while increasing the temperature. IR-TPD for the $NH_4^+$ band intensity (Figure 6) was almost analogous to the MS-measured ammonia TPD, thus proving that the acid sites were predominantly Brønsted type. However, the recovery behavior of the negative OH band during the elevation of temperature showed a shift of the band. As shown in Figure 7a, a negative absorption was observed at 3603 cm$^{-1}$ at 373 K, but the position shifted gradually to a lower wavenumber, 3574 cm$^{-1}$ at 773 K.

The shift of the negative OH band was confirmed in Figure 7b, that is, wavenumber corrected spectra, showing that am-

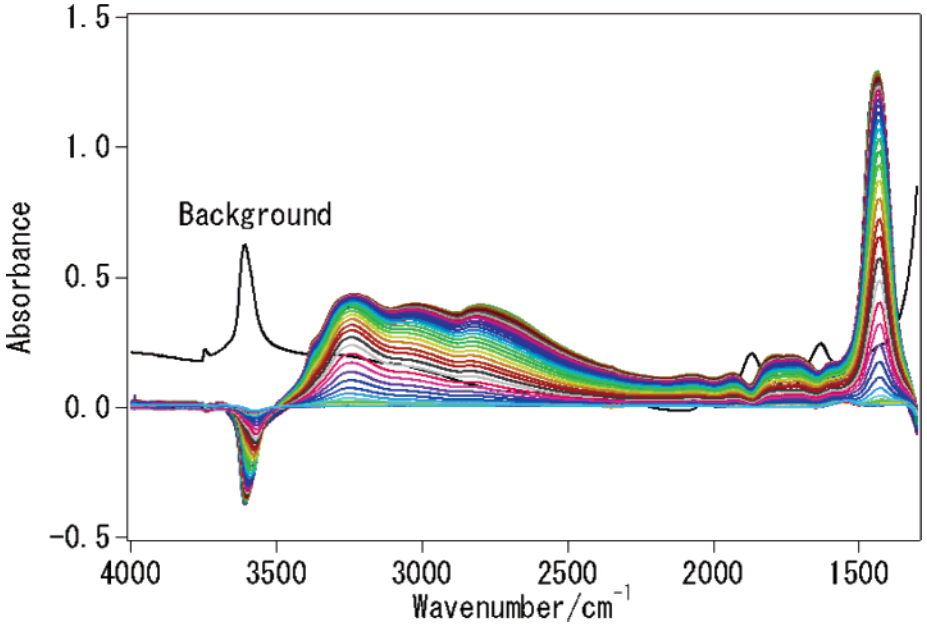


**Figure 5.** Difference spectra of ammonia on the in situ prepared HM-15 during the elevation of temperature from 373 to 773K. Background spectrum was obtained at 373 K before the adsorption of ammonia.

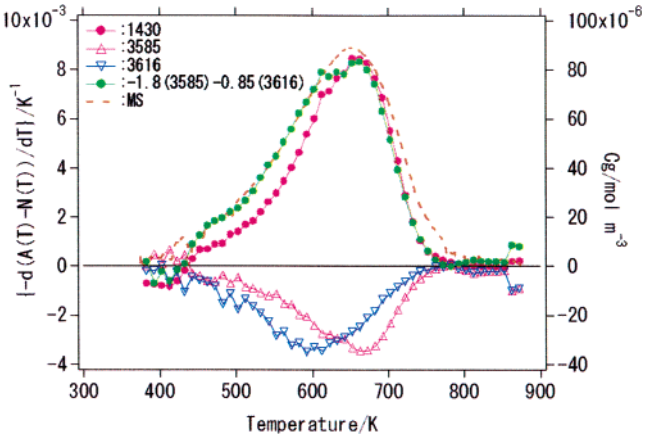


**Figure 6.** IR-TPD of ammonia on the in situ prepared HM-15 for the $NH_4^+$ and OH bands shown in the corner and MS-TPD (change of desorbed ammonia concentration, Cg) for a comparison.

monia was adsorbed on different types of OH with different strengths. Obviously, the weaker Brønsted acid site is located at the OH showing the band at a high wavenumber, and the stronger one at the low wavenumber. From the corrected spectra in Figure 7b, one kind of the OH band ascribable to the stronger Brønsted acid site was identified at 3585 cm$^{-1}$. However, another weaker OH band was identified at 3616 cm$^{-1}$; the band position was clearly identified on $NH_4$NaM ($NH_4$ exchange degree, 31%) on which only the weaker OH exists (vide infra). Furthermore, the shape of OH band in the corrected spectra did not depend on the measurement temperature, as shown in Figure 7b. Therefore, IR-TPD for two kinds of OH were calculated at the positions of 3585 and 3616 cm$^{-1}$, as shown in Figure 6. The sum of the two spectra of IR-TPD of OH was similar to MS-TPD, after these were multiplied by appropriate coefficients, that is, 1.8 and 0.85 for IR-TPD of OH at 3585 and 3616 cm$^{-1}$, respectively. Thus, it was found that not only IR-TPD of $NH_4^+$ but also MS-TPD was related to the two kinds of OH band. In other words, two kinds of Brønsted OH exist in mordenite, on which ammonia is adsorbed as $NH_4^+$. The reciprocal of adopted coefficient corresponds to extinction coefficient of OH bands, and the relative ratio, 1/1.8 : 1/0.85, almost agrees with ratio of the reported values,[11] 1.55 and 3.50 cm $\mu$mol$^{-1}$ for OH at 3584 and 3602 cm$^{-1}$, respectively.

In previous literature, OH bands of mordenite are identified at 3612 and 3575 cm$^{-1}$ as those located in the 12- and 8-MRs of the mordenite structure, respectively.[10−12] Therefore, based on the above finding, it is concluded that the Brønsted acid site on 8-MR is stronger than that on 12-MR. Furthermore, it is recognized that the Brønsted acid site is located at the 8-MR, mainly because the MS-TPD and IR-TPD of $NH_4^+$ have a relation closer to the IR-TPD of the OH band on the 8-MR at 3585 cm$^{-1}$; this is quantified more exactly in the following.

In the present study, the amount and strength of the Brønsted acid site were measured quantitatively. To do so, we simulated[2] IR-TPD spectra of two kinds of OH bands on the basis of the theoretical equation. As described above, $\Delta S$ of 47 J K$^{-1}$ mol$^{-1}$ upon desorption of ammonia (phase transformation) was assumed as a parameter required for the simulation. Furthermore, it was defined that two kinds of Brønsted OH at 3616 and 3585 cm$^{-1}$ are the sites with different strengths $\Delta H$ and amounts $A_0$, respectively; and the sum of the simulated TPD should be fitted to the IR-TPD of $NH_4^+$ as well as to MS-TPD. As shown in Figure 8, the simulated IR-TPD spectra of OH bands were fitted to the experimentally observed ones, and the sum of them fitted to MS-TPD, satisfactorily. Thus, the amounts and strengths of the two kinds of Brønsted acid sites were determined for in situ prepared HM-15 (99% of exchange level), as summarized in Table 1. It was found, therefore, that the Brønsted acid sites were located in 8-MR more than in 12-MR, and the strength of the Brønsted acid site in the 8-MR was larger than that of the site located in the 12-MR.

**IRMS-TPD on the Partially Ion-Exchanged Mordenites.** The technique of IRMS-TPD was then applied to the $NaNH_4$-mordenites with exchange degrees of $NH_4^+$, 64 to 7%. The bending vibration of $NH_4^+$ was observed at 1430 to 1440 cm$^{-1}$ throughout the samples. As decreasing the exchange level of the $NH_4^+$ cation, the OH band not only changed the intensity but also shifted the band position (Figure 9). OH bands were, like in the 99% $NH_4$-mordenite, analyzed by dividing them into

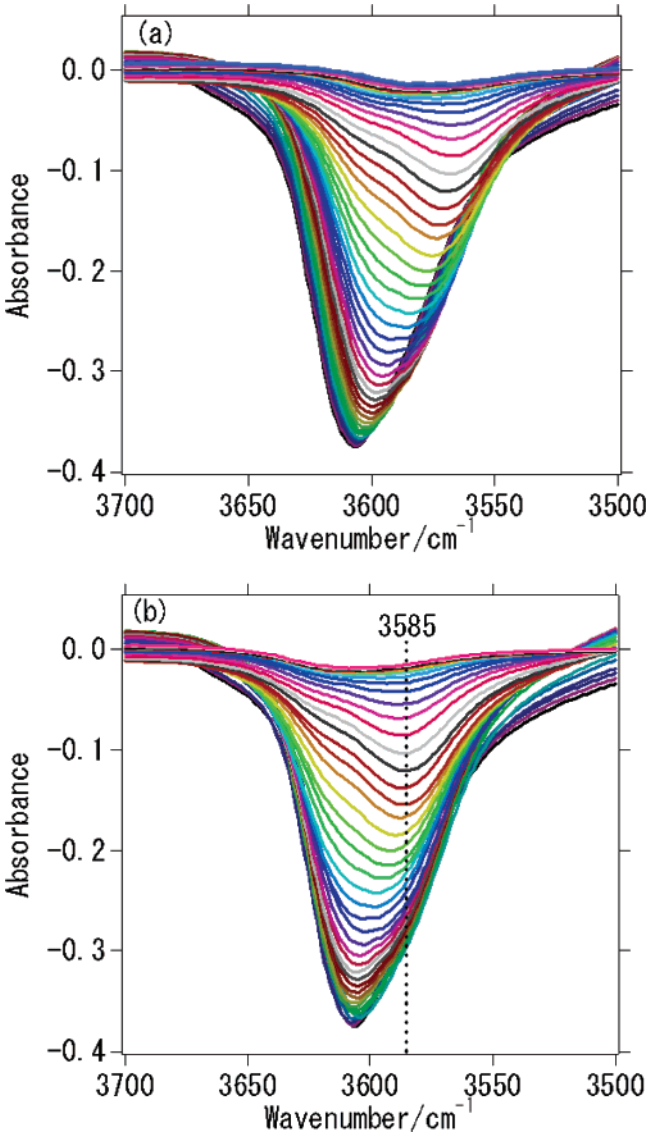


**Figure 7.** Enlarged portion of OH band in Figure 4 (a, upper) and the corrected spectra using the eq 1 (b, lower).

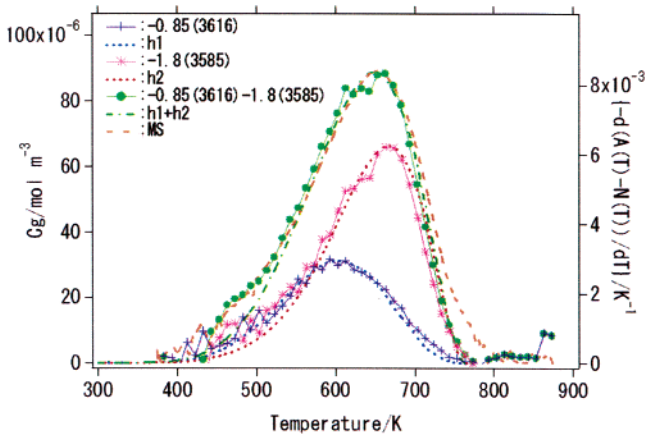


**Figure 8.** Comparison of the simulated spectra of IR-TPD with the experimentally observed corrected IR-TPD at 3616 and 3585 cm$^{-1}$. $-0.85*I_{3616}$ and $-1.8*I_{3585}$ are fitted to the simulated ones (h1 and h2), respectively, and sum of those IR-TPD and sum of simulated ones (h1 + h2) are fitted to the MS-TPD.

two absorption bands, except for the 31 and 7% $NH_4^+$-mordenites, because in these cases only one kind of OH band was observed.

**TABLE 1: Amount and Strength of Brønsted Acid OH on Mordenite with Different $NH_4^+$ Exchange Levels**

| | OH in 12-MR | | OH in 8-MR | | |
|---|---|---|---|---|---|
| $NH_4^+$ % | $A_0$ mol kg$^{-1}$ | $\Delta H$ [a] kJ mol$^{-1}$ | $A_0$ mol kg$^{-1}$ | $\Delta H$ [a] kJ mol$^{-1}$ | $A_0$ total mol kg$^{-1}$ |
| 99 | 0.42 | 147(9) | 0.77 | 155(8) | 1.19 |
| 64 | 0.40 | 146(8) | 0.42 | 150(7) | 0.82 |
| 47 | 0.41 | 145(8) | 0.10 | 153(8) | 0.51 |
| 31 | 0.37 | 143(7) | 0 | | 0.34 |
| 7 | 0.15 | 142(8) | 0 | | 0.15 |

[a] Value in parentheses shows deviation of the acid strength $\Delta H$ in kJ mol$^{-1}$.

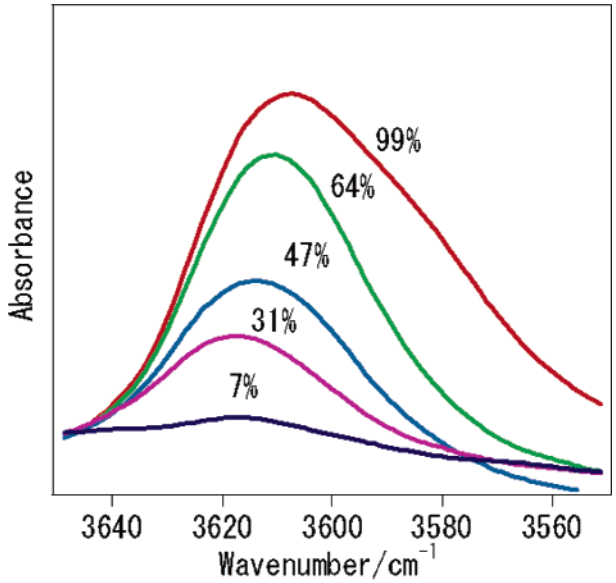


**Figure 9.** OH bands measured at 373 K before the adsorption of ammonia, N (373 K), with varying degrees of $NH_4^+$ exchange shown in the Figure.

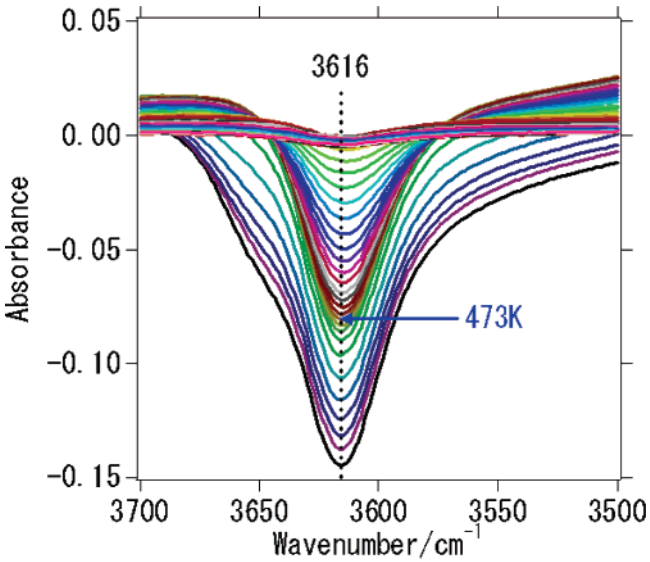


**Figure 10.** Corrected difference spectra using eq 1 observed on $NaNH_4$-mordenite ($NH_4^+$ cation exchange degree, 31%).

As a typical experimental result, the corrected difference spectra of the OH band on the $NaNH_4$-mordenite ($NH_4^+$ exchange degree, 31%) were shown in Figure 10. It was found that only one kind of OH existed at 3616 cm$^{-1}$, and the shape of the OH was independent of the measurement temperature above 473 K. The broad OH band below 473 K was caused by the so-called *l*-peak ammonia, described below. The OH band

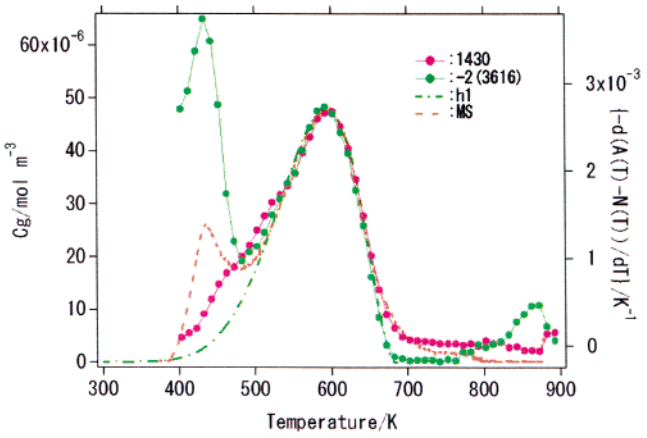


**Figure 11.** Comparison between MS-TPD, simulated spectrum of ammonia TPD (h1), IR-TPD of $NH_4^+$ at 1430 $cm^{-1}$, and IR-TPD of OH at 3616 $cm^{-1}$ multiplied by −2.

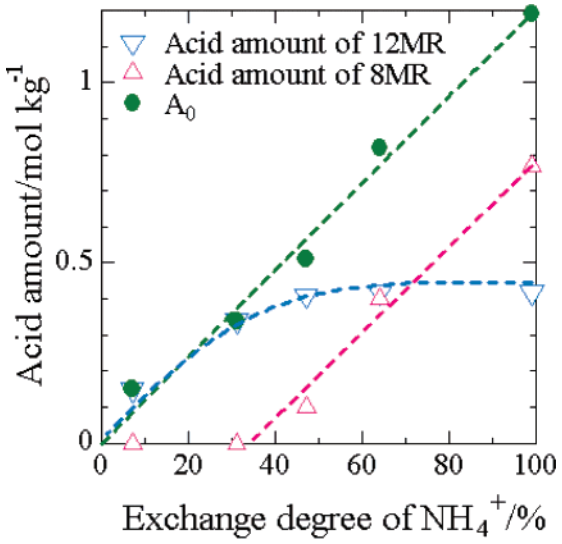


**Figure 12.** Amounts of acid site situated on 8- and 12-member rings against the degree of $NH_4^+$ exchange.

at 3616 $cm^{-1}$ was identified as OH located in 12 MR, and the change of intensity was analyzed, as shown in Figure 11. IR-TPD of $NH_4^+$ bending was almost similar to MS-TPD, and it was also related with corrected IR-TPD of OH bands; therefore, the above conclusions were applicable to these partially cation-exchanged mordenites.

MS-TPD on the highly Na-containing mordenite showed desorption of ammonia at ca. 410 K, as shown in Figure 11, which was named *l*-peak and regarded as ammonia adsorbed on the Na cation; the intensity of the *l*-peak increased with an increase in the concentration of Na cations. As shown in Figure 11, the *l*-peak could be related to the IR-TPD of OH band at 3616 $cm^{-1}$ because desorption of ammonia at ca. 410 K recovered the intensity of this band. A sharp absorption at 1650 $cm^{-1}$ was observed in the background spectrum, N (373 K), and the band intensity changed upon adsorption and desorption of the *l*-peak ammonia. It was therefore considered that ammonia was adsorbed on $Na^+$ and simultaneously interacted with OH. This type of ammonia is thereby considered not directly related with the Brønsted acidity, and therefore, the TPD profiles ascribable to the *l*-peak desorption were disregarded for the simulation.

By simulation procedures, we calculated the strength and amount of Brønsted OH, as shown in Table 1. The strength of

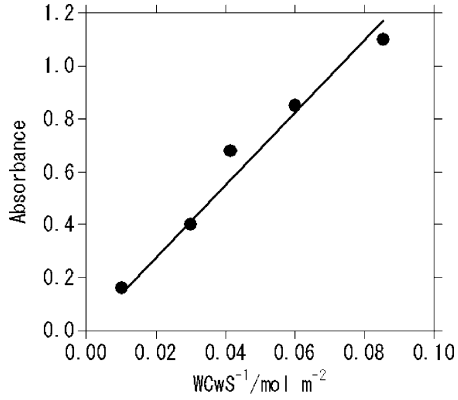


**Figure 13.** Determination of extinction coefficient of the $NH_4^+$ bending vibration band.

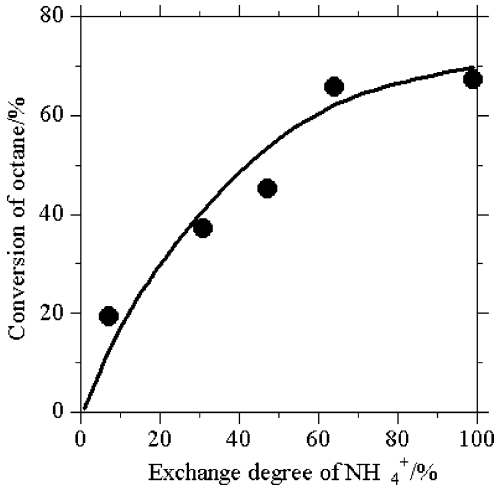


**Figure 14.** Conversion of octane 1 min after the reaction against the exchange degree of $NH_4^+$.

the acid site, $\Delta H$, was almost constant, independent of the degree of $NH_4^+$ cation exchange, and averaged values were 153 and 145 kJ $mol^{-1}$ for Brønsted acid sites situated on 8-MR and 12-MR, respectively. A simple conclusion should be noted that the smaller wavenumber is due to the stronger acidity of the Brønsted OH groups, consistent with the weaker OH bond that should induce the stronger protonation ability.

However, the amount and distribution of acid sites depended strongly on the exchange degree, as shown in Figure 12. With increasing the degree of $NH_4^+$ exchange, acid sites increased preferentially in the 12-MR, and saturated at more than 30% of the exchange degree. Acid sites situated on the 8-MR were observed only at exchange degrees higher than 30%, and the amount exceeded that on the 12-MR at more than 70%.

**Extinction Coefficient for Bending Vibration of $NH_4^+$.** According to the Lambert−Beer equation, the absorbance, *A*, for adsorbed $NH_4^+$ can be described as

$$A = \epsilon cl = \epsilon \frac{w}{S} c_w$$

where *c* and *l* are concentrations of the measured species and thickness of the sample, respectively. Because we measure the species adsorbed on a solid, *c* is replaced by ($c_w d$), ($c_w$, weight-based concentration in mol $kg^{-1}$ and *d*, density), and *l* is replaced by $w/(Sd)$ (*w*, weight of the sample and *S*, cross sectional area). The absorbances, *A*, for the bending vibration of $NH_4^+$ measured at 373 K on five kinds of $NH_4$Na-mordenite were therefore plotted against $wc_wS^{-1}$ in Figure 13, and $\epsilon$ was determined 13.7

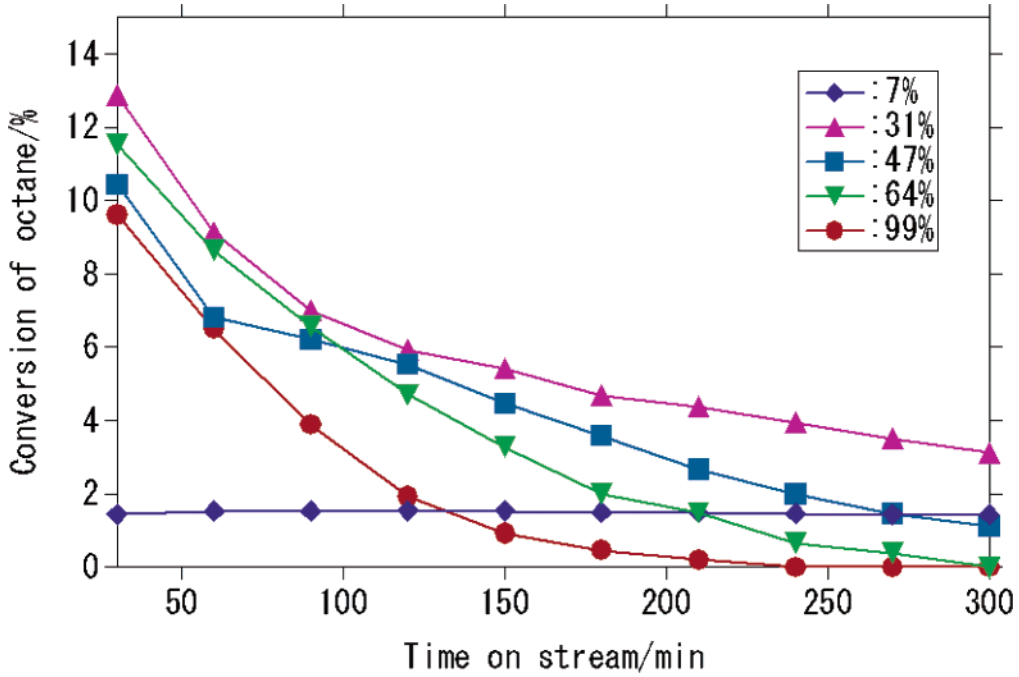


**Figure 15.** Change of catalytic activity with time-on-stream on various $NH_4Na$-mordenites with the exchange degree of $NH_4^+$ shown in the inset.

$m^2\ mol^{-1}$ from the linear relation. Thus, the obtained value of extinction coefficient almost agrees with that reported on mordenite[21] (14.7 $m^2\ mol^{-1}$).

**Catalytic Activity for Cracking of Octane.** Figure 14 shows the catalytic activity for octane cracking on in situ prepared NaH-mordenites measured 1 min after the start of the continuous flow reaction. The catalytic activity measured in the early stage increased almost proportionally with the exchange degree of $NH_4^+$. However, activities declined rapidly as shown in Figure 15. Deactivation of the catalytic activity was fast on the mordenites with high degrees of $NH_4^+$ exchange but became small on 31% of the exchange degree. The activity on 7% $NH_4$-mordenite was clearly different from others, because it did not decline for 300 min at all. At 300 min after the reaction, activities on 31 and 7% $NH_4$-exchanged mordenites were higher than those on other mordenites. Therefore, the deactivation behavior correlated well with the distribution of acid sites; on the catalysts with slow deactivation behavior (31 and 7% $NH_4$-exchanged mordenites), acid sites were preferentially located on the 12-MR, as shown above. In summary, the acid sites on the 8-MR possessed higher activity on the initial stage of the reaction, whereas the sites on the 12-MR were relatively inactive, but hardly declined by time on stream. A higher catalytic activity for hexane cracking on the acid sites located on the 8-MR of mordenite was also reported by Lukyanov et al.[22]

**DFT Calculation of the Adsorption of Ammonia.** Generally, adsorption energies are overestimated, when a local density approximation (LDA) such as VWN functional is used. However, in this study, VWN functional was used for all calculations to reduce the computational cost because the aim of the calculation in this study is to evaluate the difference in acid strengths qualitatively.

The geometry of the structure of H-mordenite was first optimized. The ammonia adsorption energy on the Brønsted acid site was then calculated using a DMol[3] program. Calculations were made for $NH_4^+$ adsorbed on four kinds of Brønsted acid sites (Figure 16) because four different T sites exist in mordenite. Thus, the calculated $NH_3$ adsorption energy depended on the location of Al in the mordenite structure, and it was larger on the $T_3$ site in 8-MR than on the $T_1$, $T_2$, and $T_4$ sites in 12-MR, as shown in Table 2. Therefore, the DFT calculation supported the difference in strengths of acid sites, measured in the present study.

## Discussion

**Distribution of Acid Strength.** In the present study, the acidity of mordenite was studied by a method of IRMS-TPD of ammonia. By utilizing a unique and useful property of the method, the Brønsted acid sites were measured quantitatively. Because there were two kinds of Brønsted acid sites, which depended on the structure of mordenite, the strengths and amounts were measured individually on each crystallographically specific site. Such a precise analysis on the distribution of acid sites has not been reported previously. Therefore, interesting findings about the acidity of zeolite were obtained in the present investigation.

The assignment of OH bands at high and low wavenumbers for those on 12-MR and 8-MR, respectively, was deduced from adsorption experiments of ammonia and pyridine probes[10−12]. Ammonia interacted with both hydroxyls, whereas pyridine adsorption diminished the intensity of the OH band located at a high wavenumber only. Therefore, the assignment of the OH band location is widely accepted. OH bands in the 4- or 5-MR (side pocket) of the mordenite structure, however, neither exist nor are detectable in the IR spectra. Although a recent study by Marie et al.[14] suggested the presence of a third Brønsted OH, the present study could not find any evidence to prove it.

However, distribution of the strengths of acidity is a matter of controversy. Zholobenko et al. reported that the acidity of Brønsted OH situated on 8-MR was stronger than that on 12-MR on the basis of a study using an ammonia probe.[10] However, Wakabayashi et al. drew a contradictory conclusion[12] because adsorption of the $N_2$ probe decreased the intensity of the OH band on 12-MR only; therefore, they concluded that, because of its stronger acidity, $N_2$ interacted with OH on the 12-MR only. Datka et al. measured the extinction coefficient of OH bands[11] and found a larger value for the OH of 12-MR; because

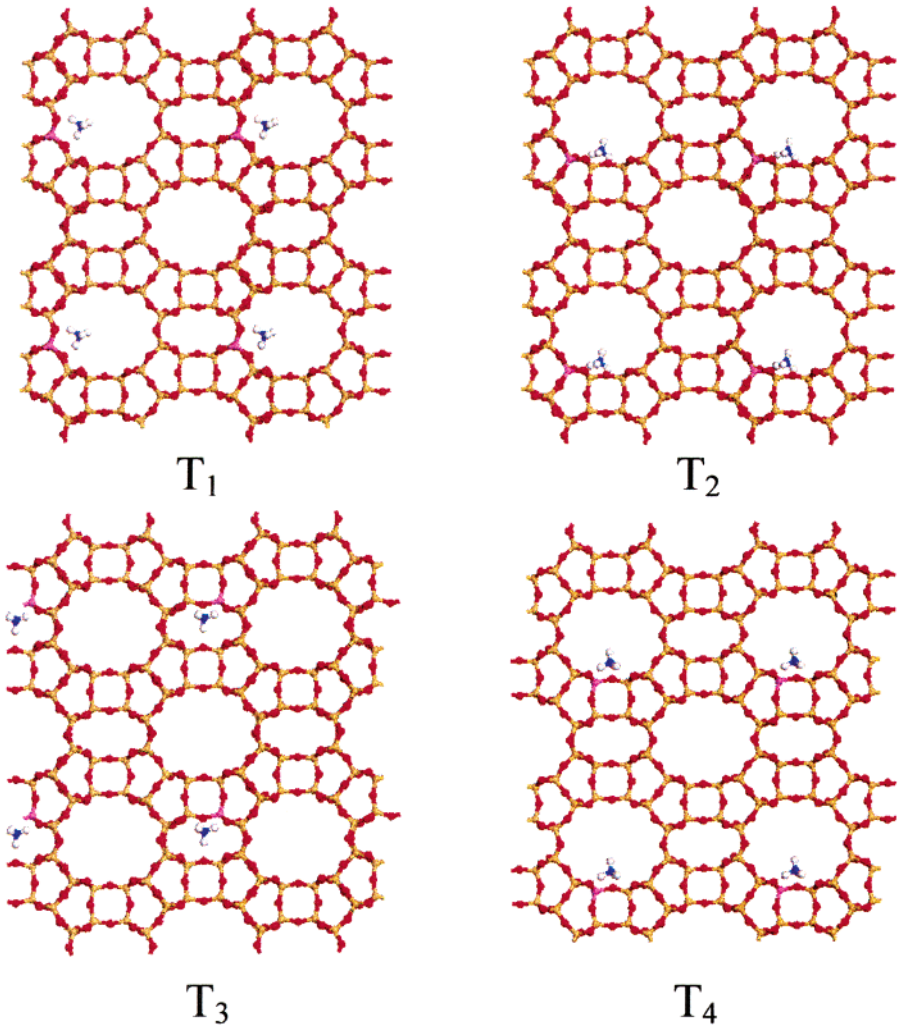


**Figure 16.** Optimized structures of $NH_4^+$ bonded to $T_1-T_4$ sites.

**TABLE 2: Heat of Ammonia Adsorption ($\Delta H$) Calculated by Dmol[3]**

| $T_{site}$ | $T_1$ | $T_2$ | $T_3$ | $T_4$ |
|---|---|---|---|---|
| $-\Delta H_{NH_3}$ (kJ/mol) | 215 | 213 | 235 | 220 |

the stronger OH was reported to have a larger value of extinction coefficient, they identified the stronger acidity of hydroxyl in the large pore.

In the present study, ammonia was used as a probe and the stronger acidity of OH on 8-MR was derived, in consistent with Zholobenko et al.[10] Contradictory conclusions seem to have derived largely because of the selected probe molecule. The adsorption of nitrogen by Wakabayashi et al. was performed at a low temperature such as ca. 100 K,[12] and this may be a reason for the different conclusion. However, here we point out the following priority of findings in the present investigation.

(1) IRMS-TPD of ammonia is a method to follow the thermal behavior of adsorbed $NH_4^+$ and hydroxyl bands directly, and therefore, with this method, information of the strength of each acid site is obtained precisely.

(2) Ammonia is a small molecule; therefore, ammonia can enter into small pores with relatively low steric hindrance. All of the acid sites responsible for the catalytic reaction were counted in the experiment of ammonia TPD, as shown by the agreement between the numbers of acid sites and Al atoms in the framework[2]. Steric hindrance for adsorption can therefore be disregarded.

(3) The OH group shows the IR absorption band at the position that reflects the strength of acidity.[23] Particularly in the region of a high wavenumber above 3600 $cm^{-1}$, the weaker OH band is located at the higher wavenumber. Therefore, the general trend observed in the band position of OH supports the present conclusion.

(4) The DFT calculation supports the conclusion of the stronger acidity of the OH located on 8-MR.

**Location of Acid Sites.** Distribution of the Brønsted OH depended on the degree of $NH_4^+$ exchange. At the low ion-exchange degree ($NH_4^+/Na^+$ ratio), the acid sites were preferentially located on the 12-MR. The Na cation on the site of 12-MR may be easily accessible with $NH_4^+$ in the solution because of less-steric hindrance. The cation at the 8-MR site was exchanged by increasing the ion-exchange degree. A high preference of Brønsted OH on the 8-MR was observed in the almost 100% $NH_4^+$-exchanged mordenite. This should show the preferential distribution of Al on the 8-MR.

According to an X-ray study by Alberti[9] on the position of Al in a natural mordenite sample with a Si/Al ratio, ca. 5, $T_3$ and $T_4$ sites in the 4-MR were the richest in Al. The position of Brønsted OH was not determined directly, because four oxygen atoms bonded to one Al cation, and the neighboring OH was directed toward one of the attached member rings. The population of Brønsted OH was therefore estimated from a comparison with spectroscopic data reported previously, and about the same probability of the OH population

in the 12- and 8-MR was proposed on the basis of the spectroscopic data.

Datka et al.[11] measured IR bands of OH on the in situ prepared H-mordenite calcined at 830 K after adsorption of pyridine, accessible only to OH in the large pore, to discriminate between OH groups situated on two member rings. They reported populations of OH on 12- and 8-MR were almost the same, that is, 3.0 and 3.5 $H^+$/unit cell, respectively.

Wakabayashi et al.[12] made a peak deconvolution of OH bands of H-mordenite; the relative ratio of the integrated absorbances of OH bands was 32:25 for bands at 3616 and 3590 $cm^{-1}$, as seen in their experimental data. The extinction coefficients of OH bands at 12- and 8-MR were reported to be 3.50 and 1.55 cm $\mu mol^{-1}$, respectively, according to Datka et al,[11] and we also used similar corresponding parameters for the curve fitting, as mentioned above (Figures 6 and 8). Concentrations of OH situated on 12- and 8-MR are therefore in a ratio of approximately 9:16, the reported values of $\epsilon$ being taken as parameters. The relative ratio thus estimated is almost in agreement with that measured in the present study on 99% $NH_4$-mordenite. The relative concentration of hydroxyls can be measured correctly from IR spectroscopy, when extinction coefficients are provided. One does not become aware of the shoulder-like OH at a lower wavenumber because of the large width of the absorption.

Recently, Kato et al.[24] reported that mordenite synthesized in the presence of a fluoride ion had a unique distribution of Al cation in the framework; based on the experiment observation and theoretical considerations, aluminum was located only on the T site in the 12-MR. As found in the present study, the location of the Brønsted OH depended strongly on the concentration of an Na cation. Therefore, various conditions of the synthetic procedure and included cation may have an influence on the final position of OH in mordenite.

**Catalysis on Acid Site on Mordenite.** Mordenite is known as the zeolite with a large pore channel of 12-MR, and the presence of the strong acid site is remarkable as well. However, the Brønsted acid sites with a strength of 153 kJ $mol^{-1}$ are located on the 8-MR, a smaller pore of the mordenite structure, as mentioned above. The conclusion has a big impact on the understanding of the catalysis in mordenite.

As found in the present study, the catalytic activity of octane cracking declined rapidly on the mordenite with a high concentration of stronger acid sites located at the position of 8-MR, whereas only the mordenite with weaker acid sites on the 12-MR showed a slow deactivation behavior. The correlation between the acid strength and the catalytic life could be explained easily because coking occurs easily on the strong acid sites, leading to the deactivation. The strong acidity and small steric capacity of 8-MR may cause the rapid deactivation of the acid sites because plugging by polymerized species occurs easily in the small pore. The stable activity on the 7% $NH_4$Na-mordenite observed in the present study suggests a possible way of modifying the catalyst life.

**Acknowledgment.** We wish to express our thanks to Professors Akira Miyamoto and Momoji Kubo of Tohoku University for their discussion of the DFT calculation of the strength of acid sites.

## References and Notes

(1) Niwa, M.; Katada, N.; Sawa, M.; Murakami, Y. *J. Phys. Chem.* **1995**, *99*, 8812.
(2) Katada, N.; Igi, H.; Kim, J. H.; Niwa, M. *J. Phys. Chem. B* **1997**, *101*, 5969.
(3) Katada, N.; Kageyama, Y.; Niwa, M. *J. Phys. Chem. B* **2000**, *104*, 7561.
(4) Katada, N.; Takeguchi, T.; Suzuki, T.; Fukushima, T.; Inagaki, K.; Tokunaga, S.; Shimada, H.; Sato, K.; Oumi, Y.; Sano, T.; Segawa, K.; Nakai, K.; Shoji, H.; Wu, P.; Tatsumi, T.; Komatsu, T.; Masuda, T.; Domen, K.; Yoda, E.; Kondo, J. N.; Okuhara, T.; Kageyama, Y.; Niwa, M.; Ogura, M.; Matsukata, M.; Kikuchi, E.; Okazaki, N.; Takahashi, M.; Tada, A.; Tawada, S.; Kubota, Y.; Sugi, Y.; Higashio, Y.; Kamada, M.; Kioka, Y.; Yamamoto, K.; Shouji, T.; Arima, Y.; Okamoto, Y.; Matsumoto, H. *Appl. Catal., A: Gen.*, in press.
(5) Sauer, J.; Ugliengo, P.; Garrone, E.; Saunders, V. R. *Chem. Rev.* **1994**, *94*, 2095.
(6) Simperler, A.; Bell, R. G.; Foster, M. D.; Gray, A. E.; Lewis, D. W.; Anderson, M. W. *J. Phys. Chem. B* **2004**, *108*, 7152.
(7) Elanany, M.; Koyama, M.; Kubo, M.; Selvam, P.; Miyamoto, A. *Microporous Mesoporous Mater.* **2004**, *71*, 51.
(8) Alberti, A.; Davoli, P.; Vezzalini, G. *Z. Kristallogr.* **1986**, *175*, 249.
(9) Alberti, A. *Zeolites* **1997**, *19*, 411.
(10) Zholobenko, V. L.; Makarova, M. A.; Dwyer, J. *J. Phys. Chem.* **1993**, *97*, 5962.
(11) Datka, J.; Gil, B.; Kubacka, A. *Zeolites* **1996**, *17*, 428.
(12) Wakabayashi, F.; Kondo, J.; Wada, A.; Domen, K.; Hirose, C. *J. Phys. Chem.* **1993**, *97*, 10761.
(13) Geobaldo, F.; Lamberti, C.; Ricchiardi, G.; Bordiga, S.; Zecchina, A.; Palomino, G. T.; Arean, C. O. *J. Phys. Chem.* **1995**, *99*, 11167.
(14) Marie, O.; Massiani, P.; Starzyk, F. T. *J. Phys. Chem. B* **2004**, *108*, 5073.
(15) Niwa, M.; Nishikawa, S.; Katada, N. *Microporous Mesoporous Mater.* **2005**, *82*, 105.
(16) Kohn, W.; Sham, L. J. *J. Phys. Rev., A* **1965**, *140*, 1133.
(17) Delley, B. *J. Chem. Phys.* **2000**, *113*, 7756.
(18) Vosko, S. H.; Wilk, L.; Nusair, M. *Can. J. Phys.* **1980**, *58*, 1200.
(19) Sawa, M.; Niwa, M.; Murakami, Y. *Zeolites* **1990**, *10*, 307.
(20) Zecchina, A.; Marchese, L.; Bordiga, S.; Paze, C.; Gianotti, E. *J. Phys. Chem. B* **1997**, *101*, 10128.
(21) Datka, J.; Gil, B.; Kubacka, A. *Zeolites* **1995**, *15*, 501.
(22) Lukyanov, D. B.; Vazhnova, T.; Cascib, J. L.; Birtill, J. J. 13th International Congress on Catalysis, Paris, P1-457, 2004.
(23) Jacobs, P. *Catal. Rev.—Sci. Eng.* **1982**, *24*, 415.
(24) Kato, M.; Itabashi, K.; Matsumoto, A.; Tsutsumi, K. *J. Phys. Chem. B* **2003**, *107*, 1788.